

## MICROSTRUCTURAL AND ELASTIC PROPERTIES OF THE EXTRACELLULAR MATRICES OF THE SUPERFICIAL ZONE OF NEONATAL ARTICULAR CARTILAGE BY ATOMIC FORCE MICROSCOPY

Rupal V. Patel, Jeremy J. Mao

*Departments of Orthodontics and Bioengineering MC 841, University of Illinois at Chicago, 801 S. Paulina Street, Chicago, IL*

### TABLE OF CONTENTS

1. Abstract
2. Introduction
3. Materials and Methods
  - 3.1. Sample Preparation
  - 3.2. Surface topographic imaging with the atomic force microscope
  - 3.3. Dynamic indentation and force spectroscopy
  - 3.4. Data Analysis and statistics
4. Results
5. Discussion
6. Acknowledgments
7. References

### 1. ABSTRACT

The structural and mechanical properties of the superficial zone of articular cartilage are not well understood. Most previous studies have focused on the overall properties of articular cartilage in the adult. In the present work, the extracellular matrices of the superficial zone of the jaw-joint condyle in the 7-day-old rabbit were subjected to dynamic indentation with atomic force microscopy (AFM). The surface topography of four equally divided regions of the entire articular surface lacked substantial variations, with mean roughness from 95.4 nm ( $\pm 28.0$ ) to 130.1 nm ( $\pm 13.8$ ). Indentations of the articular surface and the microdissected, orthogonal transverse surface revealed a narrow distribution of Young's moduli ranging from 0.92 MPa ( $\pm 0.12$ ) to 1.02 MPa ( $\pm 0.22$ ). These rather uniform structural and mechanical properties of the superficial zone of the neonatal articular cartilage are in contrast to our previous finding of a gradient distribution of Young's moduli of the superficial zone of adult articular cartilage from 0.95 ( $\pm 0.06$  MPa) to 2.34 ( $\pm 0.26$  MPa) (Hu et al.: J Struct Biol 2001:136:46-52), indicating that the mechanical properties of the articular surface are modified during development. Thus, articular cartilage's anisotropic mechanical properties may be specific to the adult, rather than the neonatal. It is further postulated that the structural and mechanical properties of the superficial zone of articular cartilage are regulated by chondrocytes in addition to their unidirectional development pathway toward subchondral bone formation.

### 2. INTRODUCTION

The articulating surfaces of the diarthrodial joint consist of cartilage. The surface layer of articular cartilage

is called superficial zone (SZ) or lamina splendens, and usually composed largely of extracellular matrix (SZ Figure 1) (2). The SZ is of considerable importance because it forms structural constraints of wear and tear of the joint surface in both normal function and pathologic status such as osteoarthritis (3-6). Underneath the superficial zone are progenitor cells surrounded by fine tangential fibers, followed by hypertrophic chondrocytes (P and H in Figure 1). Chondrocytes are recognized to have a unidirectional development pathway from the superficial zone toward hypertrophy and apoptosis, followed by replacement with angiogenesis and osteogenic cells (Figure 1). Despite these morphological observations, the growth mechanisms of articular cartilage are not well understood. For example, it is not clear how the structural and mechanical properties of the superficial zone of articular cartilage are maintained and regulated (2,7-10).

Scanning electron microscopy (SEM) has been the major tool for studying the morphological features of the SZ of articular cartilage. Surface irregularities such as pits, ridges and humps identified with SEM (11-14) were later confirmed to vary up to approximately 1000 nm with atomic force microscopy (AFM) in humeral joints of young adult cows (15). Recently, we found that surface topography of the fibrocartilaginous SZ of the adult rabbit jaw joint varied up to approximately 2000 nm (1), twice as high as hyaline articular cartilage (15). In addition, we observed a gradient distribution of Young's moduli among different regions of the adult SZ (1), approximately two fold higher for the anterior regions than the posterior regions. However, it is not clear whether these regional differences in structural and mechanical properties are intrinsic or gradually evolve during development.

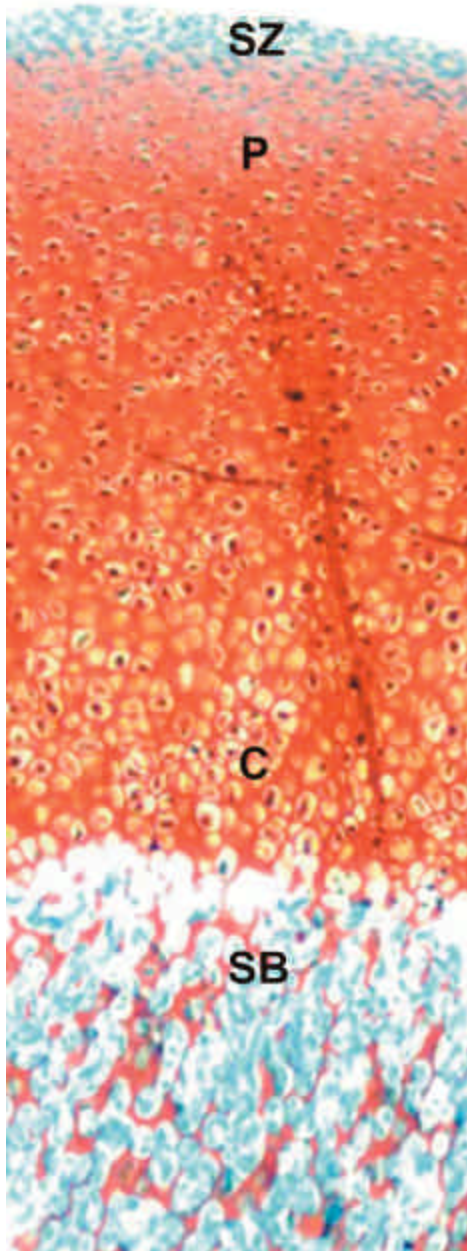


**Figure 1. A:** Histological image of articular cartilage of the mandibular condyle in the 7-day-old NZW rabbit. The superficial zone (SZ) is characterized by a thin layer composed of mostly the extracellular matrix. Immediately underneath the SZ are progenitor cells in the proliferating zone (P), followed by hypertrophic chondrocytes (H). It is recognized that articular chondrocytes develop from progenitor cells to eventual hypertrophy and apoptosis, and are replaced by subchondral bone (SB) in a unidirectional process. It is not clear how structural and mechanical properties of the superficial zone are maintained and regulated. A model is proposed in Fig. 8 to postulate that the superficial zone is actively maintained and regulated by chondrocytes during development in addition to their unidirectional developmental pathway toward subchondral bone. 20  $\times$ ; Safranin O and fast green counter stain.

Recently, a finite element model based on quantitative polarized light microscopy data has demonstrated dependence of mechanical properties of the SZ on its thickness (16). This is of further interest because the thickness of articular cartilage is known to vary with age (17).

AFM has several advantages over conventional electron microscopy in studying the superficial zone of articular cartilage (1,15). First, AFM allows characterization of thin materials such as the SZ over the rest of articular cartilage. Previous material characterization of cartilage has largely been limited to the entire cartilage samples (18,19). Second, AFM enables regional analysis of the SZ so that potential differences among different regions can be revealed (1). Third, AFM allows observation of surface topographic features with nanometer resolution, which reveals finer structures that may not be seen with other imaging tools (1,15). Fourth and perhaps most importantly, AFM can be used as a nanoindentation device to detect micromechanical properties of the SZ (1) whose primary function is to withstand mechanical stresses. By using dynamic indentation with AFM to probe different regions of the extracellular matrices of the SZ of the neonatal articular cartilage in the present work, we tested the hypothesis that the SZ of neonatal articular cartilage has homogenous structural and mechanical properties. Our data demonstrate that the extracellular matrices of the SZ in different regions of the neonatal articular surface indeed possess not only uniform distribution of topographic characteristics, but also nearly isotropic elastic properties. These homogenous structural and elastic properties of the neonatal articular surface are in sharp contrast to our previous finding of a gradient distribution of these structural and mechanical properties across the articular surface in the adult age (1), suggesting that the structural and mechanical properties of the neonatal articular surface are modified during development. Based on these findings, we further postulate that the structural and mechanical properties of the superficial zone of articular cartilage are regulated by chondrocytes in addition to their unidirectional development pathway toward subchondral bone formation.

## 3. MATERIALS AND METHODS

### 3.1. Sample preparation

A total of 18 left and right jaw joint condyles of 9 normal, seven-day-old, New Zealand White rabbits were harvested within 15 min of euthanasia. After dissecting the condylar head transversely at the level of the condylar neck, microdissection was applied to divide the articulating surface into four regions: anteromedial (AM), anterolateral (AL), posteromedial (PM), and posterolateral (PL) under a dissection microscope (Figure 2). A whole thickness cartilage sample per region including the subchondral bone (cf., Figure 1), approximately  $0.7 \times 0.7 \times 2$  mm<sup>3</sup> (length $\times$ width $\times$ height) in size, was microdissected (Figure 2B). The sample's bony surface was rapidly dried and glued to a circular glass slide using fast-drying cyanoacrylate (Measurements Group, Raleigh, NC). Then,

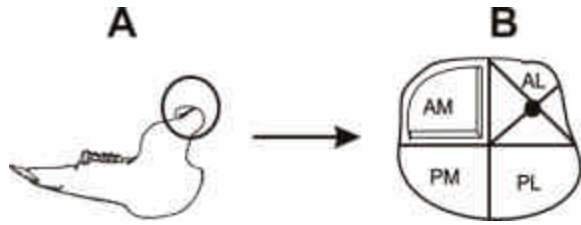


**Figure 2.** Sagittal view of the rabbit mandibular condyle (circled in A) and the superior view of the articular surface (B). The articular surface was divided and dissected into the four regions: anteromedial (AM), anterolateral (AL), posteromedial (PM) and posterolateral (PL). A whole thickness articular cartilage sample, approximately  $0.7 \times 0.7 \times 2 \text{ mm}^3$  in size including subchondral bone, was harvested in each region (B) for further sample preparation for atomic force microscopy. The 3D view of the AM region illustrates sample harvest. For each region, the center of the cross point as illustrated in the AL region (B) was selected for AFM scanning. The bony surface was rapidly dried and glued to the AFM disk, which was then mounted to the AFM piezoscanner. The articular surface was exposed and hydrated with PBS for AFM scanning and indentation.

the glass slide was fixed onto a stainless steel disk using two-sided adhesive tape, which was subsequently mounted on the atomic force microscope (AFM) piezoscanner. During these procedures, the sample was constantly irrigated with phosphate-buffered saline. The present work was approved by the Animal Care Committee of the University of Illinois at Chicago.

### 3.2. Topographic imaging of articular surface with atomic force microscope

Topographic imaging was performed by probing the extracellular matrices in the geometric center of each of the four regions ( $5 \times 5 \mu\text{m}$  scan sizes; cf., Figure 2B) on the articular surface using contact-mode AFM at a scanning frequency of 1 Hz (Nanoscope IIIa, Veeco-Digital Instruments, Santa Barbara, CA). Cantilevers with a nominal force constant of  $k = 0.12 \text{ N/m}$  and oxide-sharpened  $\text{Si}_3\text{N}_4$  tips were used. The radius of curvature of the scanning tips was 20 nm. The mean surface roughness was quantified by using the following equation:

$$R_a = \frac{\sum_{i=1}^N |Z_i - Z_{cp}|}{N}$$

where  $Z_{cp}$  is the Z value of the center plane,  $Z_i$  is the current Z value and N is the number of points within a given area (1).

### 3.3. Dynamic indentation and force spectroscopy

The AFM scanning tip was calibrated against glass slide carriers used as the substrate for cartilage samples. Upon indentation of the intercellular matrices of cartilage samples and concurrent scanning, scan size was set to be  $5 \times 5 \mu\text{m}$ . Force mapping involved data acquisition of indentation force and the corresponding

displacement in the Z plane during both extension and retraction of the cantilever tip at a frequency of 14 Hz. Upon completion of force spectroscopy for axial indentation on the articular surface, each sample was bisected perpendicular to the articular surface at its geometric center, and remounted onto another glass slide. The corresponding bisected surface of the SZ,  $90^\circ$  to the articular surface, was exposed for indentation and force spectroscopy in 14 condyles in the same fashion as described above. The elastic modulus (E) was calculated from force spectroscopy data by following the Hertz model (20-22). As the AFM tip deflected to and from the sample's surface, it encountered various features and yielded electrical potential to the piezoscanner. Consequently the piezoscanner either retracted or extended in response to the resulting electrical potential. For each sample, the average Young's modulus was derived from individual calculations of randomly selected points of the force-volume (FV) map using the following equation (20-22):

$$E = \frac{3F(1-\nu)}{4\sqrt{R}\delta^{3/2}}$$

where E is the Young's modulus, F is the applied mechanical load,  $\nu$  is the Poisson ratio that was assumed to be 0.30 (17), R is the radius of curvature of the AFM tip, and  $\delta$  is indentation depth.

### 3.4. Data analysis and statistics

The raw measurements of the elastic modulus (E) for the left and right condyles were first subjected to Student T tests to determine whether they differed between the left and right sides. Once a lack of statistical significance between the left and right condyles was established, all the data between the left and right sides were pooled for each of the four corresponding regions. All surface roughness and the Young's modulus data were subjected to the Analysis of Variance (ANOVA) with Bonferroni adjustment to determine whether they differed significantly among and between the four regions at an alpha level of 0.05.

## 4. RESULTS

The superficial zone (SZ) of the neonatal articular cartilage was smooth, pale and uniform with no indication of surface defect or degeneration under the stereomicroscope. The articular surface observed with AFM was largely acellular, and had an apparently random distribution of peaks and valleys. No surface irregularities such as pits, ridges and humps were observed. Representative topographic images of the extracellular matrices in the AM, AL, PM and PL regions are illustrated in Figure 3. Quantification of surface topography revealed a rather uniform distribution of mean surface roughness, varying from  $95.4 \text{ nm} (\pm 28.0)$  to  $130.1 \text{ nm} (\pm 13.8)$  among the AM, AL, PM and PL regions (Figure 4). There was a lack of significant differences in surface roughness among the 4 regions.

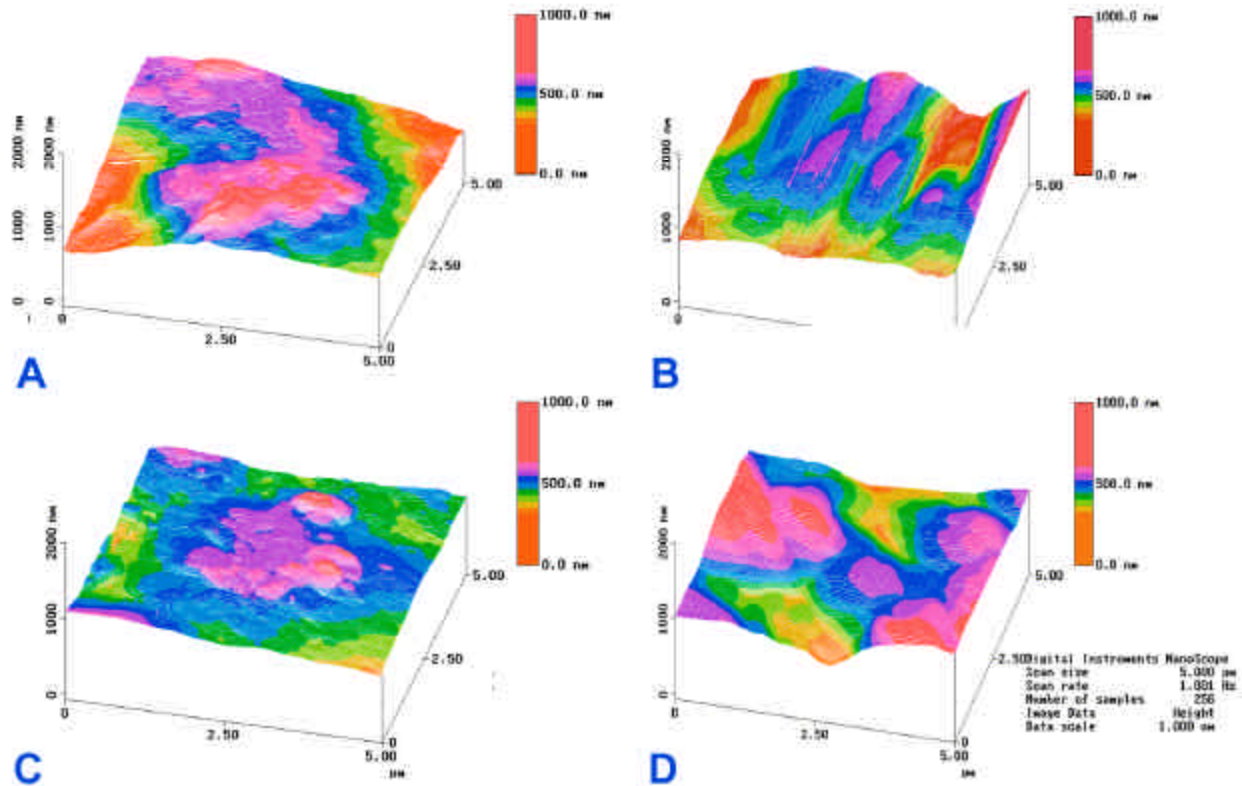


**Figure 3.** Representative topographic images of the (A) anteromedial, (B) anterolateral, (C) posteromedial, and (D) posterolateral regions of the superficial zone of neonatal articular cartilage in  $5 \times 5 \mu\text{m}$  scans. The Z depth of surface topography is rather uniform among these regions.

A typical FV image is illustrated in Figure 5. The volume image in Figure 5A demonstrates distribution of peaks and valleys in the Z range of a few hundred nanometers. FV image in (B) captured in three dimensions shows the deflection of the AFM tip in given Z positions from which force plots (Figure 5C) were selected from. The deflection of the cantilever tip was plotted as it approached and retracted from the sample surface during extension and retraction of the piezoscanner (Figure 5C).

Indentation in the axial direction (perpendicular to the articular surface) revealed a narrow range of Young's moduli among the AM, AL, PM, and PL regions: from  $0.95 \text{ MPa} (\pm 0.15)$  to  $1.02 \text{ MPa} (\pm 0.22)$ . The corresponding Young's moduli for transverse indentation (orthogonal to the articular surface) were from  $0.92 \text{ MPa} (\pm 0.12)$  to  $1.01 \text{ MPa} (\pm 0.26)$ . For either the axial or transverse indentation, the differences in Young's moduli among the four regions were not statistically significant ( $p > 0.05$ ), suggesting intrinsically homogenous capacity of the neonatal articular surface to sustain biomechanical stresses among its various regions (Figure 6). These Young's modulus data were verified by a lack of statistical significance in the differences of the average Young's moduli of the left and right condyle samples (data not shown). The apparent isotropic properties among the four regions of the neonatal articular surface were in sharp contrast to a gradient distribution of the anisotropic properties in the superficial

zone of the adult articular cartilage (Figure 7), from the highest AM region ( $2.34 \pm 0.26 \text{ MPa}$ ) to the lowest PL region ( $0.95 \pm 0.06 \text{ MPa}$ ) (1). The Young's moduli of the AM and AL regions of the neonatal articular surface were significantly smaller than the AM and AL regions of the adult articular surface ( $p < 0.01$ ) (Figure 7), suggesting their different capacities to withstand mechanical stresses.

## 5. DISCUSSION

In contrast to approximately 50% reductions in surface roughness from the anterior to posterior regions of the adult articular cartilage (1), the surface roughness of the neonatal articular surface is rather uniform. The roughness of the adult articular SZ is approximately 2 to 3 fold higher than the neonatal (cf.,1). The presently observed structural adaptation is indirectly supported by changes in both collagen and glycosaminoglycan contents in the mouse jaw-joint condyle within weeks after birth (23), and overall histological changes of the tibial articular cartilage from newborn to young adult rabbits (24).

Mechanical analysis of the SZ of the neonatal articular cartilage indicates remarkable homogeneity, as evidenced by homogenous distribution of Young's moduli among various regions. The homogenous distribution of the Young's moduli among the four arbitrarily and equally divided regions of the neonatal SZ suggests that the



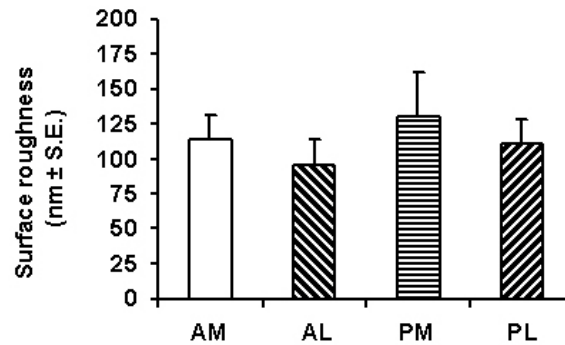


**Figure 4.** Mean surface roughness of the superficial zone of neonatal articular cartilage showed homogenous distribution among the anteromedial (AM), anterolateral (AL), posteromedial (PM) and posterolateral (PL) regions in  $5 \times 5 \mu\text{m}$  scans. The mean surface roughness varied from 95.4 nm ( $\pm 28.0$ ) to 130.1 nm ( $\pm 13.8$ ). Differences in mean surface roughness among the four regions lacked statistical significance ( $p > 0.05$ ).

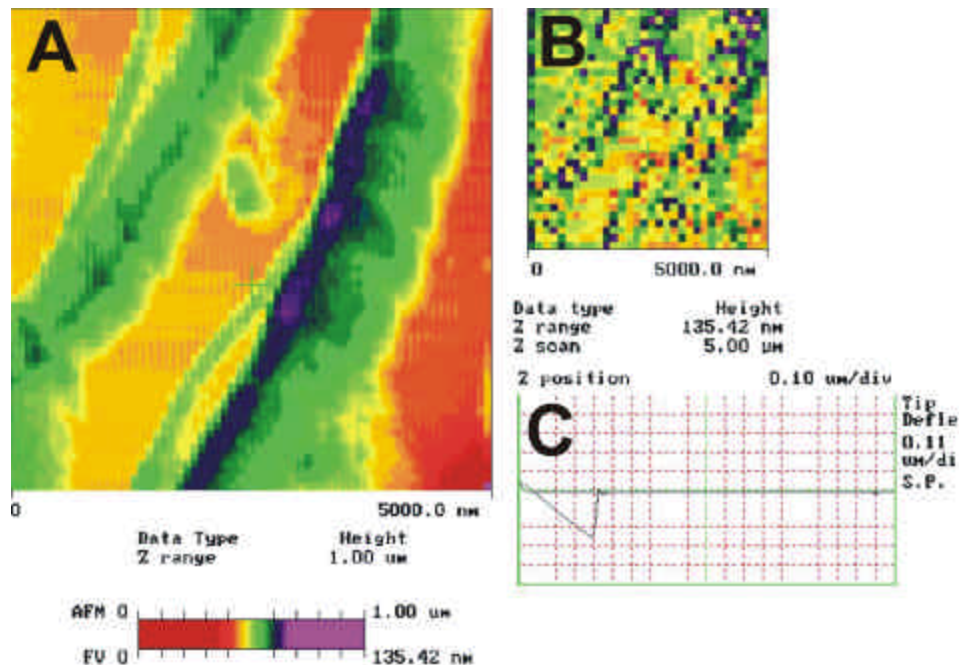


**Figure 5.** Representative force-volume (FV) images and the resulting force curve. A: Volume image of surface topography demonstrated peaks and valleys in the Z range of a few hundred nanometers. FV image in (B) showed the deflection of the AFM tip in given Z positions from which force plots (C) were selected from. The deflection of the cantilever tip was plotted as it approached and retracted from the sample surface during extension and retraction of the piezoscanner (C).

neonatal articular surface has nearly uniform stress-bearing capacities. The contrast between rather homogenous distribution of Young's moduli in the neonatal articular surface and our previous finding of a gradient distribution of Young's moduli in the adult articular surface (1) suggests that the neonatal articular surface is a dynamic matrix during development and maturation (Figure 7). Thus, articular cartilage's anisotropic mechanical properties may be specific to the adult, rather than the neonatal.

The present data must be interpreted with the following caveats. First, indentation was made in the extracellular matrix, instead of chondrocytes. The

presently identified mechanical properties therefore reflect those of the matrices rather than cells or composite properties of both. Second, indentation was performed in small areas whereas conclusion was drawn for the superficial zone of the entire articular surface. Although each microdissected articular sample is small (approximately  $0.7 \times 0.7 \times 2 \text{ mm}^3$ ), there is room for overgeneralization of the structural and mechanical properties of the entire articular surface. Further division of the entire articular surface into finer samples is obviously exhaustive. These limitations would have been more significant if absolute mechanical properties are of interest.

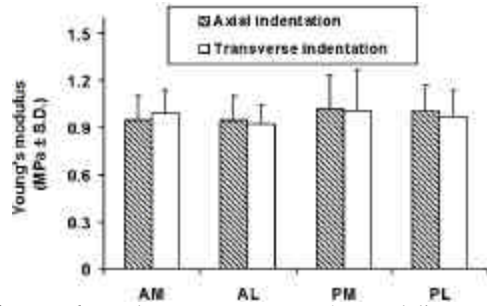


**Figure 6.** The average Young's moduli among the anteromedial (AM), anterolateral (AL), posteromedial (PM) and posterolateral (PL) regions. Oblique bars: axial indentation of the superficial zone of articular cartilage surface. Open bars: transverse indentation of the corresponding location that was orthogonal to the axial indentation. In either case, there was a lack of statistically significant differences in Young's moduli among the 4 regions ( $p > 0.05$ ).

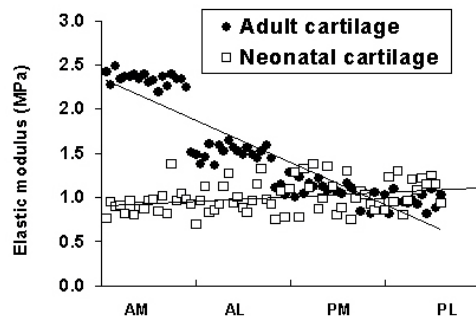


**Figure 7.** Comparison of the present data of Young's moduli of the neonatal articular surface (open squares) with the adult articular surface (solid circles) in Hu et al. (1). AM and AL regions of the adult articular surface showed significantly higher Young's moduli ( $p < 0.01$ ) than corresponding regions of the neonatal cartilage.

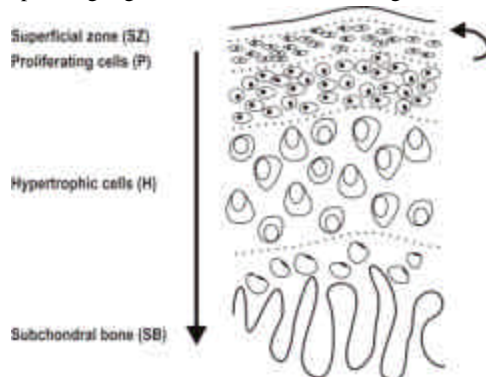


**Figure 8.** Schematic diagram of a model that postulates that the superficial zone of articular cartilage is regulated by chondrocytes in addition to their commonly recognized unidirectional development process toward subchondral bone. The downward arrow indicates chondrocytes' unidirectional development pathways. This postulate is based on the differences in the structural and mechanical properties of the superficial zones between the neonatal articular cartilage observed in the present work and those of adult articular cartilage in Hu et al. (1). Note that different cartilage zones correspond to the histology of articular cartilage in Figure 1.

The parallel increases in structural and mechanical properties of articular surface, evident from the present data and Hu et al. (1), indicate that structural and mechanical properties of articular surface are coregulated during its maturation process, presumably by both intrinsic and extrinsic factors. The most plausible extrinsic factor responsible for the significantly higher Young's moduli of the anterior region than the corresponding region of the neonatal articular surface appears to be weaning, a developmental milestone that changes mechanical usage of the articular surface of the jaw joint (25). The monumental increase in mechanical demand by weaning on the jaw-joint articular cartilage can perhaps be regulated by either micromechanical stresses experienced by the articular condyle or via cellular synthesis of extracellular matrix molecules. The first possibility of direct micromechanical stresses, although plausible, likely only accounts for instantaneous changes in extracellular matrix structures (8,9,26). Changes in cellular synthesis of extracellular matrix molecules as a result of gene upregulation triggered by micromechanical stresses are likely responsible for sustained structural changes in the articular surface seen as differences in structural properties between the present data and Hu et al. (1). This potential mechanism is consistent with postnatal enhancement of mechanical stiffness and proteoglycan content of articular cartilage due to increasing compressive stresses (27-30) and can be illustrated in Figure 8. Cartilage cells undergo phenotypic changes from the progenitor zone, which is immediately underneath the articular surface, to increasingly mature chondrocytes deeper in the proliferating and hypertrophic zones in a unidirectional development process (the downward arrow in Figure 8). The articular surface appears to be dynamically maintained by chondrocytes that reside immediately underneath, shown as the counter-clockwise, curved arrow extending from the progenitor cell zone to the superficial zone in Figure 8, in addition to their recognized unidirectional development process towards cartilage replacement by subchondral bone. Recently, the resting zone of growth plate cartilage has been demonstrated to contain stem-like cells that are responsible for morphogenesis of the remaining cartilage (31). This dynamic regulation of the articular surface can perhaps be considered a part of appositional growth of articular cartilage (10). It is further postulated that the structural and mechanical properties of the superficial zone of articular cartilage are regulated by chondrocytes in addition to their unidirectional development pathway toward subchondral bone formation.

## 6. ACKNOWLEDGMENTS

We are grateful to Drs. Robert Scapino and Charles Turner for their critical review of early versions of the manuscript. We thank three anonymous reviewers whose comments helped to improve the quality of our manuscript. Priya Radhakrishnan and Kai Hu are acknowledged for their technical assistance. Tejas Joshi is acknowledged for processing histological sections such as shown in Figure 1. This research was supported by a Biomedical Engineering Research Grant from the Whitaker Foundation and NIH grants R01DE13964 and R15DE13088.

## 7. REFERENCES

1. Hu K., P. Radhakrishnan, R.V. Patel & J.J. Mao: Regional structural and viscoelastic properties of fibrocartilage upon dynamic nanoindentation of the articular condyle. *J Struct Biol* 136, 46-52 (2001)
2. Williams P.L., L.H. Bannister, M.M. Berry, P. Collins, M. Dyson, J.E. Dussek, M.W.J. Ferguson: *Gray's Anatomy*. Churchill Livingstone: Edinburgh, 450-452 (1995)
3. Hunziker E.B., A. Ludi & W. Herrmann: Preservation of cartilage matrix proteoglycans using cationic dyes chemically related to ruthenium hexammine trichloride. *J. Histochem Cytochem.* 40, 909-917 (1992).
4. Mow V.C., A. Ratcliffe & A.R. Poole: Cartilage and diarthrodial joints as paradigms for hierarchical materials and structures. *Biomaterials* 13, 67-97 (1992)
5. Oloyede A. & N.D. Broom: A physical model for the time-dependent deformation of articular cartilage. *Connect Tissue Res* 29, 251-261 (1993)
6. Oloyede A. & N.D. Broom: Stress-sharing between the fluid and solid components of articular cartilage under varying rates of compression. *Connect Tissue Res* 30, 127-141 (1993)
7. Serafini-Fracassini A. & J.W. Smith: *The Structure and biochemistry of cartilage*. Churchill Livingstone: Edinburgh. pp. 45-54 (1974)
8. Broom N.D. & H. Silyn-Roberts: The three-dimensional 'knit' of collagen fibrils in articular cartilage. *Connect Tissue Res* 23, 261-277 (1989)
9. Setton L.A., W. Zhu & V.C. Mow: The biphasic poroviscoelastic behaviour of articular cartilage: role of the surface zone in governing the compressive behaviour. *J Biomech* 26, 581-592 (1993)
10. Hayes A.J., S. MacPherson, H. Morrison, G. Dowthwaite & C.W. Archer: The development of articular cartilage: evidence for an appositional growth mechanism. *Anat Embryol* 203, 469-479 (2001)
11. Bloebaum R. D. & A.S. Wilson: The morphology of the surface of articular cartilage in adult rats. *J Anat* 131, 333-346 (1980)
12. Ghadially F.N: *Fine Structure of the Synovial Joints. A Text and Atlas of the Ultrastructure of Normal and Pathological Articular Tissues*. Butterworth: London (1983)
13. Helminen H. J., J.S. Jurvelin, M. Tammi, A. Peltari, C.M. Svartback, I. Kiviranta, A.M. Saamanen, & K. Paukkonen: Prolonged ethanol replacement by CO<sub>2</sub> increases splits on articular cartilage surface after critical point drying. *J Microsc* 137, 305-312 (1985)
14. Kirk T.B., A.S. Wilson & G.W. Stachowiak: The morphology and composition of the superficial zone of mammalian articular cartilage. *J Orthop Rheum* 6, 21-28 (1993)
15. Jurvelin J.S., D.J. Muller, M. Wong, D. Studer, A. Engel & E.B. Hunziker: Surface and subsurface morphology of bovine humeral articular cartilage as assessed by atomic force and transmission electron microscopy. *J Struct Biol* 117, 45-54 (1996)
16. Korhonen R.K., M. Wong, J. Arokoski, R. Lindgren, H.J. Helminen, E.B. Hunziker & J.S. Jurvelin: Importance of the superficial tissue layer for the indentation stiffness of articular cartilage. *Med Eng Phys* 24, 99-108 (2002)
17. Athanasiou K.A., M.P. Rosenwasser, J.A. Buckwalter, T.I. Malinin & V.C. Mow: Interspecies comparisons of in situ intrinsic mechanical properties of distal femoral cartilage. *J Orthop Res* 9, 330-340 (1991)
18. Arnoczky S.P., C.A. McDevitt, M.B. Schmidt, V.C. Mow & R.F. Warren: The effect of cryopreservation on canine menisci: a biochemical, morphologic, and biomechanical evaluation. *J Orthop Res* 6, 1-12 (1988)
19. Proctor C. S., M.B. Schmidt, R.R. Whipple, M.A. Kelly & V.C. Mow: Material properties of the normal medial bovine meniscus. *J Orthop Res* 7, 771-782 (1989)
20. A-Hassan E., W.F. Heinz, M.D. Antonik, N.P. D'Costa, S. Nageswaran, C.A. Schoenenberger & J.H. Hoh: Relative microelastic mapping of living cells by atomic force microscopy. *Biophys J* 74, 1564-1578 (1998)
21. Heinz W.F. & Hoh J.H. Spatially resolved force spectroscopy of biological surfaces using the atomic force microscope. *Trends in Biotech* 17, 143-150 (1999)
22. A.B. Mathur, G.A. Truskey, & W.M. Reichert: Atomic force and total internal reflection fluorescence microscopy for the study of force transmission in endothelial cells. *Biophys J* 78, 1725-1735 (2000)
23. Livne E & M. Silbermann: Changes in the structure and chemical composition of the mandibular condylar cartilage of the neonatal mouse. *Arch Oral Biol* 28, 805-812 (1983)
24. Clark J.M., A. Norman & H. Notzli: Postnatal development of the collagen matrix in rabbit tibial plateau articular cartilage. *J Anat* 191, 215-221 (1997)
25. Weijs W.A., P. Brugman & E.M. Klok: The growth of the skull and jaw muscles and its functional consequences in the New Zealand rabbit (*Oryctolagus cuniculus*). *J Morphol* 194, 143-161 (1987)
26. Koob T.J., P.E. Clark, D.J. Hernandez, F.A. Thurmond & K.G. Vogel: Compression loading in vitro regulates

## Structural and mechanical properties of neonatal articular cartilage

proteoglycan synthesis by tendon fibrocartilage. *Arch Biochem Biophys* 298, 303-12 (1992)

27. Ahmed A. M. & D.L. Burke: In-vitro measurement of static pressure distribution in synovial joints-part I: Tibial surface of the knee. *J Biomech Eng* 105, 216-225 (1983)

28. Benjamin M.& J.R. Ralphs: Fibrocartilage in tendons and ligaments--an adaptation to compressive load. *J Anat* 193, 481-494 (1998)

29. Mao J.J., F. Rahemtulla.& P.G. Scott: Proteoglycan expression in the rat temporomandibular joint in response to unilateral bite raise. *J Dent Res* 77, 1520-1528 (1998)

30. Petersen W. & B. Tillmann: Structure and vascularization of the cruciate ligaments of the human knee joint. *Anat & Embryol* 200, 325-334 (1999)

31. Abad V, J.L. Meyers, M. Weise, R.I. Gafni, K.M. Barnes, O. Nilsson, J.D. Bacher & J. Baron: The role of the resting zone in growth plate chondrogenesis. *Endocrinology* 143, 1851-1857 (2002)

**Key Words:** Matrix, Cartilage, Chondrocyte, Structural, Mechanical, Articular

**Send correspondence to:** Dr. Jeremy Mao, Departments of Orthodontics and Bioengineering MC 841, University of Illinois at Chicago, 801 South Paulina Street, Chicago, IL 60612, Tel: 312-996-2649, Fax: 312-996-7854, E-mail: jmao2@uic.edu